

Rainfall an unlikely factor in Kīlauea's 2018 rift eruption

<https://doi.org/10.1038/s41586-021-04163-1>

Received: 5 June 2020

Accepted: 19 October 2021

Published online: 2 February 2022

 Check for updates

Michael P. Poland¹✉, Shaul Hurwitz², James P. Kauahikaua³, Emily K. Montgomery-Brown¹, Kyle R. Anderson², Ingrid A. Johanson³, Matthew R. Patrick³ & Christina A. Neal⁴

ARISING FROM J. I. FARQUHARSON & F. AMELUNG, *F. Nature* <https://doi.org/10.1038/s41586-020-2172-5> (2020)

If volcanic eruptions could be forecast from the occurrence of some external process, it might be possible to better mitigate risk and protect lives and livelihoods. Farquharson and Amelung¹ suggested that the 2018 lower East Rift Zone (ERZ) eruption of Kīlauea Volcano—the most destructive eruption in Hawai‘i in at least 200 years²—was triggered by extreme precipitation, which caused increased pore pressure that resulted in mechanical weakening of the volcano. Here we argue that Kīlauea’s 2018 eruption was instead caused by significant pre-eruptive pressurization, that pre-eruptive rainfall was not extreme, and that there is no significant correlation between rain and eruptions at Kīlauea. Understanding the causal mechanisms of volcanic eruptions is vital for hazard assessment and mitigation, and misattribution may compromise monitoring, preparedness, communication and response efforts.

Farquharson and Amelung cite, in their Author Correction³, a “lack of substantial precursory summit inflation” at Kīlauea and conclude that the 2018 lower ERZ eruption was not induced by increased magma pressure. To the contrary, visual and geodetic observations indicate that a significant increase in magma pressure began in mid-March 2018, six weeks before the eruption. The pressurization impacted the entire magmatic system and was indicated by ground deformation of up to tens of centimetres and increases of lava lake levels by tens of metres at Pu‘u‘ō‘ō (site of eruptive activity during 1983–2018) and 20 km uprift at the summit (site of eruptive activity and a lava lake during 2008–2018), as well as extension of the ERZ⁴ (Fig. 1). Although the magnitude of this deformation was less than of those preceding other historical ERZ intrusions (for example, March 2011⁵), deformation rates were higher, and the stress state of the volcano was different, implying a different failure threshold. Farquharson and Amelung¹ did not detect this pressurization because they examined interferometric synthetic aperture radar data, which suffer from temporal aliasing and can be unduly influenced by short-term transient deformation events, and the vertical components of only a few Global Navigation Satellite System (GNSS) sites, which meant that important horizontal displacements and the overall deformation expressed by the full network (Fig. 1) were missed. Pressurization was accompanied by waning lava effusion from Pu‘u‘ō‘ō, indicating a backup in Kīlauea’s plumbing system^{4,6}—a process that had previously resulted in magma-system pressurization and the formation of new eruptive vents^{5,6}.

These changes prompted the U.S. Geological Survey Hawaiian Volcano Observatory to issue Volcanic Activity Notices (VANs) on 17 and 24 April 2018, well before the onset of dyke intrusion on 30 April and eruption on 3 May. The VANs reported that transient deformation, high lava levels and an increase in shallow earthquake rates indicated an increase in magma pressure, and that this pressurization “could lead to

the opening of a new vent on or near Pu‘u‘ō‘ō”⁷. In fact, a small fissure eruption did occur on the west flank of Pu‘u‘ō‘ō on 30 April, apparently just before magma began moving downrift towards the lower ERZ⁴.

Lava-lake surface elevation changes provide a near-direct indication of change in magma reservoir pressure at Kīlauea⁸. In 2018, the pre-eruptive weeks-long increases in lava-lake surface heights at both the summit and Pu‘u‘ō‘ō imply pressure changes of hundreds of kilopascals that affected the entire magmatic system of the volcano. These pressure increases transferred stress to the volcanic edifice, as indicated by geodetic data. The pressure changes exceeded, by more than two orders of magnitude, the rainfall-induced pore pressure perturbation of 0.1 kPa modelled by Farquharson and Amelung¹ at a few kilometres depth, which itself is smaller than changes induced by Earth tides (-10 kPa)^{9,10}; thus, stress changes over both short (hours) and long (weeks–months) timescales far exceed those modelled as due to pore pressure variations. Further, groundwater near magma probably exists in a highly compressible multiphase (liquid and steam) or supercritical state, which would further reduce¹⁰ the very small pressure changes modelled by Farquharson and Amelung¹.

To determine precipitation, Farquharson and Amelung¹ used the NASA (National Aeronautics and Space Administration)/JAXA (Japanese Aerospace Exploration Agency) Tropical Rainfall Measuring Mission and Global Precipitation Measurement satellite datasets calibrated by comparison to a single rain gauge (Hawai‘i Volcanoes National Park (HVNP)) on the east side of Kīlauea’s summit. Data from HVNP were sparse in 2014 and 2015, and no data were collected after 2015. There are known problems with interpreting and quantifying satellite precipitation data over land, especially in coastal and island regions with high elevation and orographic influences¹¹. Rainfall decreases by about half only a few kilometres to the west of HVNP¹², which is the region covered by most of the satellite ‘pixel’ area used by Farquharson and Amelung¹ (Fig. 2a) and exemplifies the poor ability of the satellite data to capture the extreme rainfall gradients that exist. This region can receive large amounts of rainfall during both wet-season subtropical cyclone (“kona low”) events¹³ and hurricanes, which usually occur in dry-season months¹⁴, both of which also highlight the extreme temporal rainfall gradients. The ‘pixel’ does not cover Kīlauea’s ERZ, where Pu‘u‘ō‘ō, the 2018 dyke and the 2018 lower ERZ eruption site are located.

Publicly available data¹⁵ from rain gauges on the southeast portion of the Island of Hawai‘i (Fig. 2b) indicate no anomalous rainfall in the days, weeks and months before the eruption. Daily rainfall measurements are available from Hilo Airport since 1950, but a lack of daily measurements at rain gauges on the ERZ, like that in Kea‘au, permit only monthly average precipitation measurements (Fig. 2b). Most large

¹U.S. Geological Survey, Cascades Volcano Observatory, Vancouver, WA, USA. ²U.S. Geological Survey, California Volcano Observatory, Moffett Field, CA, USA. ³U.S. Geological Survey, Hawaiian Volcano Observatory, Hilo, HI, USA. ⁴U.S. Geological Survey, Volcano Science Center, Anchorage, AK, USA. ⁵e-mail: mpoland@usgs.gov

Matters arising

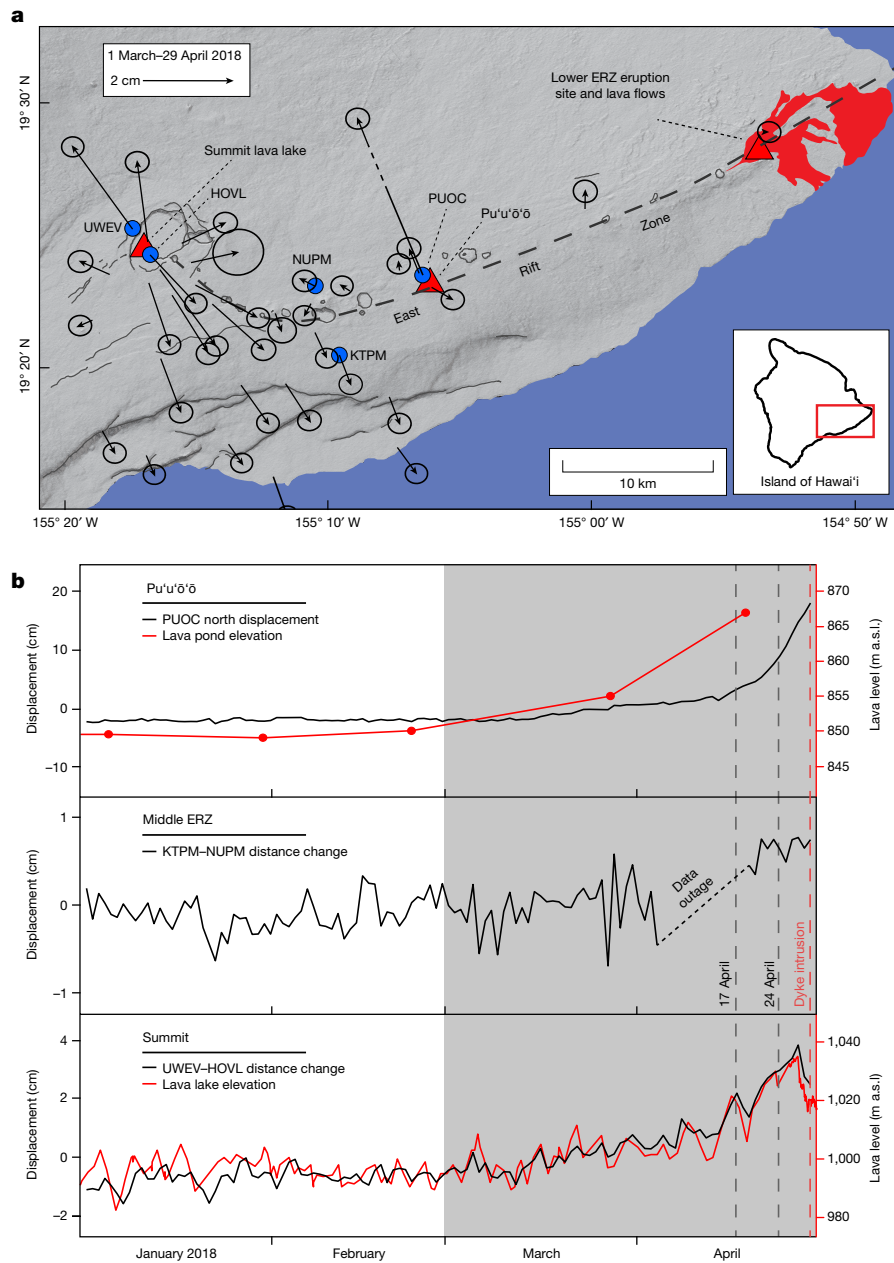


Fig. 1 | Monitoring data from Kilauea Volcano spanning January–April 2018.

a. Locations of GNSS stations shown in time series plots (blue circles), eruptive vents (red triangles), 2018 lower ERZ lava flow field (red area), major geological structures of Kilauea and GNSS displacements with 2σ error ellipses spanning 1 March–29 April 2018 (grey shaded area in time series plot). PUOC vector is not to scale. **b.** Time series plots of north displacement from GNSS site PUOC and sporadic measurements of lava pond elevation at Pu'u'o'o (top), distance

change between middle ERZ GNSS sites (middle), and continuously measured summit lava level and distance change between summit GNSS sites (bottom). Dashed vertical grey lines indicate times when VANs were issued by the U.S. Geological Survey Hawaiian Volcano Observatory. Time series plots end on 30 April, when the lower ERZ dyke initiated (red dashed vertical line); the lower ERZ eruption started on 3 May. GNSS displacements include up to a few millimetres of secular seaward motion of the volcano's south flank.

storms that affect the island last for several days and are recorded on multiple stations, including HVNP. Farquharson and Amelung¹ note that “several months of greater than average rainfall culminated in record downpour, with 1.26 m of rain falling within 24 h (14–15 April 2018) on Kaua'i (northwest of the Island of Hawai'i),” but this storm system never reached the Island of Hawai'i, as indicated by the rain gauges at Hilo Airport and elsewhere in the lower ERZ.

Perhaps more fundamentally, little of the rain that falls on Kilauea affects the ERZ. Horizontal permeability at Kilauea is typically 10–100 times greater than vertical permeability, and groundwater within the ERZ is compartmentalized, with solidified dykes parallel to the rift zone acting as low-permeability barriers to flow¹⁶. The region of heaviest

precipitation on Kilauea is east of the summit and north of the ERZ (Fig. 2a), but recharge from this rain does not flow towards Pu'u'o'o because groundwater flow, which is controlled by volcanic structure and topography, is to the east-northeast¹⁶.

The statistical analysis of Farquharson and Amelung¹ does not account for the complex patterns of rainfall and eruptions at Kilauea. The authors define a ‘wet season’ spanning 25 August–9 March (their Author Correction³) based on ~20 years of satellite data and then extrapolate back to the year 1790 in their analysis of eruption timing. Nearly 100 years of rain gauge data from across the Hawaiian Islands provide a more robust means of determining a “wet season” for the ERZ, which, on the basis of the Rainfall Atlas of Hawai'i¹², is November–April—a time

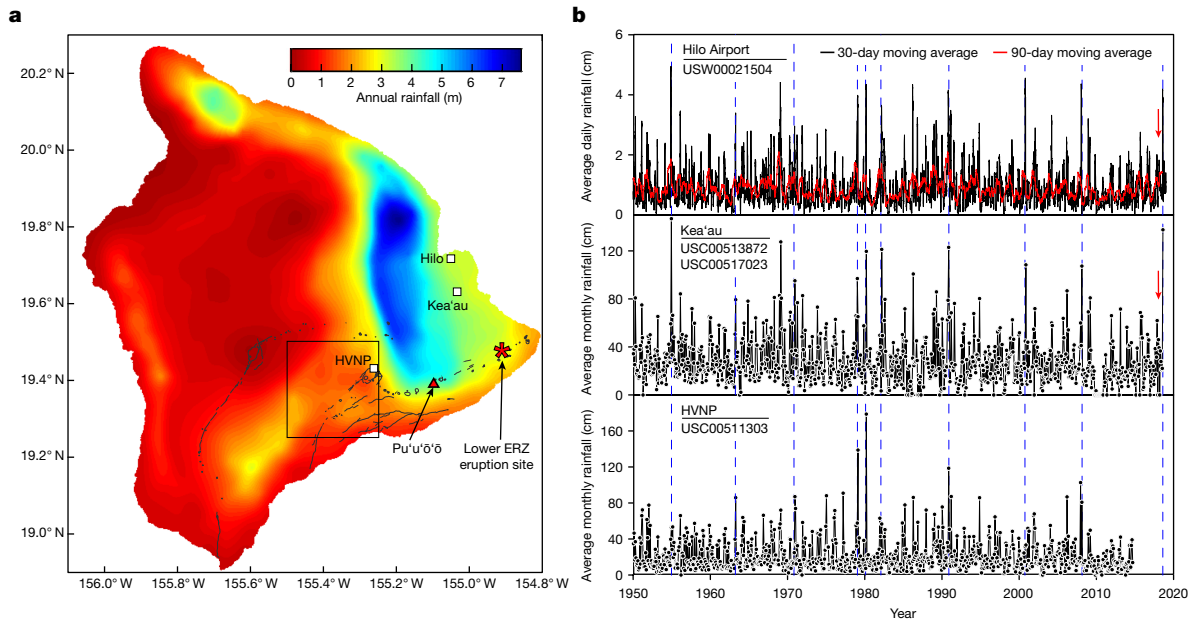


Fig. 2 | Rainfall on the Island of Hawai'i. **a**, Average annual rainfall distribution¹² showing large gradients between Kilauea summit (HVNP) and the ERZ. White squares give the locations of rain gauges near the ERZ and at Kilauea summit used in this analysis. Black box outlines satellite data pixel used by Farquharson and Amelung¹. **b**, 30- and 90-day moving daily average rainfall in

Hilo, and monthly average rainfall at Kea'au and HVNP; rain gauge numbers indicated in plots¹⁵. Periods of heavy rainfall, which can happen during any season, affect multiple gauges; a few examples are indicated by vertical dashed blue lines. Red arrow indicates onset of the 2018 lower ERZ eruption on 3 May, several months before a large storm (Hurricane Lane¹⁴) in August 2018.

during which roughly half of confirmed eruptions (33 of 61)¹⁷ occurred at Kilauea. Rainfall patterns are more nuanced than this, however; some of the雨iest periods since 1950 occurred during the May–October ‘dry season’, including one of the wettest tropical cyclones to ever strike Hawai‘i since instrumental measurements began: Hurricane Lane in August 2018¹⁴ (Fig. 2b). Moreover, there is a variable lag time between rainfall and pore pressure increase at depth. Thus, ‘wet season’ eruptions could have been triggered by rainfall in the preceding ‘dry season’ and vice versa. This is the scenario implied by the Farquharson and Amelung¹ model for the 2018 lower ERZ eruption, in which rain falling during their ‘wet season’ caused an eruption during their ‘dry season’. Finally, Farquharson and Amelung¹ point out that the onset of the 1983–2018 Pu‘u‘ō‘ō eruption (3 January 1983) was during the ‘wet season’, but that eruption was composed of dozens of individual phases, including several dyke intrusions⁵. In looking at the entirety of the Pu‘u‘ō‘ō eruptive sequence, we find, again, that roughly half of all new eruptive episodes occurred during the rain-gauge-defined ‘wet season’ for the ERZ¹². The question of rainfall triggering of eruptions is an important one but, given the subtlety of the stress effects, requires a thorough analysis of the numerous potential influences, from the state of the volcano to the rates of pore pressure diffusion.

Several studies have addressed the potential for external forces to prompt volcanic eruptions, and it is possible that subtle changes in stress induced by rainfall could affect volcanic systems that are already poised to erupt¹⁸. At Kilauea in 2018, however, magma pressure was increasing rapidly, and the magnitude of this pressure change was several orders larger than pore pressure changes conceivably caused by rainfall. In the context of the historical record, rainfall was not extreme before the eruption. The geodetic and lava lake observations were conclusive enough for the Hawaiian Volcano Observatory to issue public warnings weeks before the eruption began. Research into the influence of extrinsic forces on volcanism must clear a very high bar, ruling out intrinsic processes and avoiding observational and reporting biases¹⁹. Such research is not purely academic, but contributes directly to assessing hazards, mitigating the consequences of volcanic eruptions and communicating reliable information to affected communities.

Data availability

GNSS datasets analysed during the current study are available from the UNAVCO Geodetic Facility for the Advancement of Geosciences (GAGE) facility, <https://www.unavco.org/data/gps-gnss/gps-gnss.html>, and rainfall data are available from the National Oceanic and Atmospheric Administration National Centers for Environmental Information, <https://www.ncdc.noaa.gov/cdo-web/search>.

1. Farquharson, J. I. & Amelung, F. Extreme rainfall triggered the 2018 rift eruption at Kilauea Volcano. *Nature* **580**, 491–495 (2020).
2. Neal, C. A. et al. The 2018 rift eruption and summit collapse of Kilauea Volcano. *Science* **363**, 367–374 (2019).
3. Farquharson, J. I. & Amelung, F. Author Correction: Extreme rainfall triggered the 2018 rift eruption at Kilauea Volcano. *Nature* **582**, E3 (2020).
4. Patrick, M. R. et al. The cascading origin of the 2018 Kilauea eruption and implications for future forecasting. *Nat. Commun.* **11**, 5646 (2020).
5. Orr, T. R. et al. in *Hawaiian Volcanoes: From Source to Surface* (eds Carey, R. et al.) Vol. 208, Ch. 18, 393–420 (AGU, 2015).
6. Patrick, M., Orr, T., Anderson, K. R. & Swanson, D. Eruptions in sync: improved constraints on Kilauea Volcano’s hydraulic connection. *Earth Planet. Sci. Lett.* **507**, 50–61 (2019).
7. Hazard Notification System (HANS) for Volcanoes (USGS, accessed 3 March 2021); https://volcanoes.usgs.gov/vhp/archive_search.html
8. Patrick, M. R., Anderson, K. R., Poland, M. P., Orr, T. R. & Swanson, D. A. Lava lake level as a gauge of magma reservoir pressure and eruptive hazard. *Geology* **43**, 831–834 (2015).
9. Emter, D. in *Tidal Phenomena* (eds Wilhelm, H. et al.), 293–309 (Springer, 1997).
10. Manga, M. When it rains, lava pours. *Nature* **580**, 457–458 (2020).
11. Chen, Y., Ebert, E. E., Walsh, K. J. E. & Davidson, N. E. Evaluation of TRMM 3B42 precipitation estimates of tropical cyclone rainfall using PACRAIN data. *J. Geophys. Res.* **118**, 2184–2196 (2013).
12. Giambelluca, T. W. et al. Online rainfall atlas of Hawai‘i. *Bull. Am. Meteorol. Soc.* **94**, 313–316 (2013).
13. Caruso, S. J. & Businger, S. Subtropical cyclogenesis over the central north Pacific. *Weather Forecast.* **21**, 192–205 (2006).
14. Nugent, A. D. et al. Fire and rain: the legacy of Hurricane Lane in Hawai‘i. *Bull. Am. Meteorol. Soc.* **101**, E954–E957 (2020).
15. Climate Data Online (NOAA, accessed 3 March 2021); <https://www.ncdc.noaa.gov/cdo-web/search>
16. Hurwitz, S. et al. in *The 2008–2018 Summit Lava Lake at Kilauea Volcano, Hawai‘i* (eds Patrick, M. et al.) Ch. F, US Geological Survey Professional Paper 1867 <https://doi.org/10.3133/pp1867F> (USGS, 2021).
17. Global Volcanism Program (Smithsonian Institution, accessed 3 March 2021); <https://volcano.si.edu/volcano.cfm?vn=332010&tab=Erupptions>
18. Violette, S. et al. Can rainfall trigger volcanic eruptions? A mechanical stress model of an active volcano: ‘Piton de la Fournaise’, Reunion Island. *Terra Nova* **13**, 18–24 (2001).

Matters arising

19. Sawi, T. M. & Manga, M. Revisiting short-term earthquake triggered volcanism. *Bull. Volcanol.* **80**, 57 (2018).

Acknowledgements We are grateful for comments from S. Ingebritsen and L. Mastin.

Author contributions M.P.P., E.K.M.-B., K.R.A., I.A.J. and M.R.P. contributed to magma pressure descriptions and calculations. S.H., J.P.K. and E.K.M.-B. contributed to rainfall calculations and pore pressure impacts. C.A.N. contributed hazard assessment and communication information. M.P.P. and M.R.P. contributed to statistical arguments. M.P.P. coordinated manuscript preparation, in which all authors engaged.

Competing interests The authors declare no competing interests.

Additional information

Correspondence and requests for materials should be addressed to Michael P. Poland.

Reprints and permissions information is available at <http://www.nature.com/reprints>.

Publisher's note Springer Nature remains neutral with regard to jurisdictional claims in published maps and institutional affiliations.

© The Author(s), under exclusive licence to Springer Nature Limited 2022

Reply to: Rainfall an unlikely factor in Kīlauea's 2018 rift eruption

<https://doi.org/10.1038/s41586-021-04164-0>

Jamie I. Farquharson¹ & Falk Amelung¹

Published online: 2 February 2022

REPLYING TO M. P. Poland et al. *Nature* <https://doi.org/10.1038/s41586-020-2172-5> (2022)

 Check for updates

In the accompanying Comment¹, Poland et al. use rain gauge data to argue that, in contrast to the conclusion in our previously published paper², rainfall in the months leading up to the eruption was not anomalously high and that the eruption occurred in response to substantial magma pressurization. We demonstrate below that rain gauge data do in fact show anomalously high precipitation. Poland et al. miss this signal by looking only at the gauges furthest from the rift and by not accounting for the underlying distribution of the data. While we agree that there was precursory summit displacement (as we state in our Author Correction³) that prompted the U.S. Geological Survey to issue a Volcanic Activity Notice on 17 April, this does not necessarily suggest wholesale pressurization of the volcanic system. We show below that summit displacement was much less than before previous intrusions. Pressurization—however defined—does not preclude an external eruption trigger: eruptions are referred to as triggered^{4–7} if they are precipitated by an external force regardless of whether pre-eruptive magma pressurization is evident⁸.

Poland et al. claim that “no anomalous rainfall” is observed in nearby gauge data. There are five gauge locations in the vicinity of the rift zone at which data are available for the 2018 period (Fig. 1a). Of these, Poland et al. show data from those furthest from the rift—Hilo (repeated here: Fig. 1b, c) and two gauges near Kea’au—highlighting ten historical incidences of heightened rainfall recorded at each. However, they demonstrate no assessment of the underlying distribution of the time-averaged time series data, and provide no description of how they quantify ‘anomalous’ rainfall.

Closer to the rift, we observe the maximum recorded (data go back to 2009) daily values for two gauges in the Pahoa area (US1HHI0051 and US1HHI0003; Fig. 1a; the latter is shown in Fig. 1d, e). While we show here only gauges that cover the early 2018 period and for which super-decadal data are available, we note that 30-, 90- or 180-day maxima were also recorded by gauges at Pahoa, Kurtistown and Mountain View in the weeks before the eruption.

Further, as demonstrated in Fig. 1c, e, the underlying distributions of time-averaged rainfall are clearly non-normal; indeed, they are characterized by a lognormal distribution, as expected (rainfall cannot be negative) and as accounted for in our original Article. Any statistical evaluation of anomalous rainfall must take this distribution into account⁹; simply highlighting individual wet periods is arbitrary and unscientific. When the lognormal distribution is accounted for, the 90-day averages from both of the gauge datasets referred to by Poland et al. (Hilo and Kea’au) exhibit a $>1\sigma$ (1 standard deviation) deviation from the long-term mean before the eruption (for example, Fig. 1b for Hilo). Moreover, gauges such as those at Pahoa (Fig. 1d)—closer to the rift zone than the examples chosen by Poland et al. (Fig. 1a)—exhibit deviations of greater than 2σ from the mean in the weeks before the 2018 eruption.

Poland et al. also suggest that satellite data for a 27-km² pixel covering the summit are not representative of precipitation throughout the rift zone and that our calibration method may unduly influence data in that pixel. As described in our Article, the described calibration is an empirical factor—determined using the Hawai’i Volcanoes National Park gauge (Fig. 1a)—bringing the absolute values of recorded rainfall in line with gauge data. By definition, this does not affect relative changes within the time series and so remains unaffected by the underestimation of rainfall in coastal areas by the Tropical Rainfall Measuring Mission (TRMM)¹⁰. Moreover, uncalibrated data for the adjacent pixels also show statistically anomalous rainfall (>1 or 2σ above the mean) before the eruption (Fig. 1g–k), including pixels mostly over the ocean. Thus, statistically anomalous rainfall is observed in independent gauge and satellite data (including datasets referred to by Poland et al.). This is especially pronounced for gauge data in the immediate vicinity of the rift zone (compare Fig. 1b, c with Fig. 1d, e).

Poland et al. infer substantial pressurization of the magmatic system in the weeks before the intrusion from (i) 20 cm of displacement of a Global Positioning System (GPS) station in the Pu’u ‘ō’ō area, (ii) precursory mid-rift baseline rate change, (iii) 3- to 4-cm precursory lengthening of a summit caldera Global Positioning System baseline and (iv) lava lake level increase. The implication is that magma pressure increase reflects stress increase throughout the volcanic edifice.

(i) Around Pu’u ‘ō’ō, neither the magnitude nor the direction of displacement of GPS station PUOC is echoed in neighbouring stations (Fig. 2b, e, i), a fact that is misleadingly not reflected in Fig. 1a of ref.¹. This station—approximately 25 m from the crater’s edge—indicates shallow, highly localized changes in the system, and is clearly not representative of system deformation more broadly (for example, Fig. 2e). In fact, interferometric synthetic aperture radar (InSAR) observations show that the Pu’u ‘ō’ō area subsided (Fig. 2b, g). (ii) A detailed depiction of precursory mid-rift baseline change shows that the rate was not appreciably different to those of previous years and that there was little if any acceleration (Fig. 2m, n), in contrast to the interpolated signal of ref.¹ (their Fig. 1b). (iii) Although the horizontal GPS displacements around the northern caldera are generally consistent with the inflation of an intra-caldera source, the InSAR-observed subsidence (Fig. 2a) is not: the intrusion was precursed by transient deflation (possibly part of a deflation–inflation event) associated with subtle radial contraction and subsidence (Fig. 2h, i). This is in contrast to the situation in 2011, when InSAR data show the inflation signal above the Halema’uma’u chamber (Fig. 2c)¹¹. A more detailed comparison with previous intrusions shows that the 2018 pre-intrusion vertical and baseline displacements were 1.7–3 times lower than in 2007 and 2011 (Fig. 2l, m). Indeed, the KTPM–NUPM baseline change in the lead-up to the 2018 eruption falls inside the range of secular change recorded in the same time period in previous years (2010, 2012–2017; Fig. 2n).

¹Rosenstiel School of Marine and Atmospheric Science, University of Miami, Miami, FL, USA. [✉]e-mail: jifarq89@googlemail.com

Matters arising

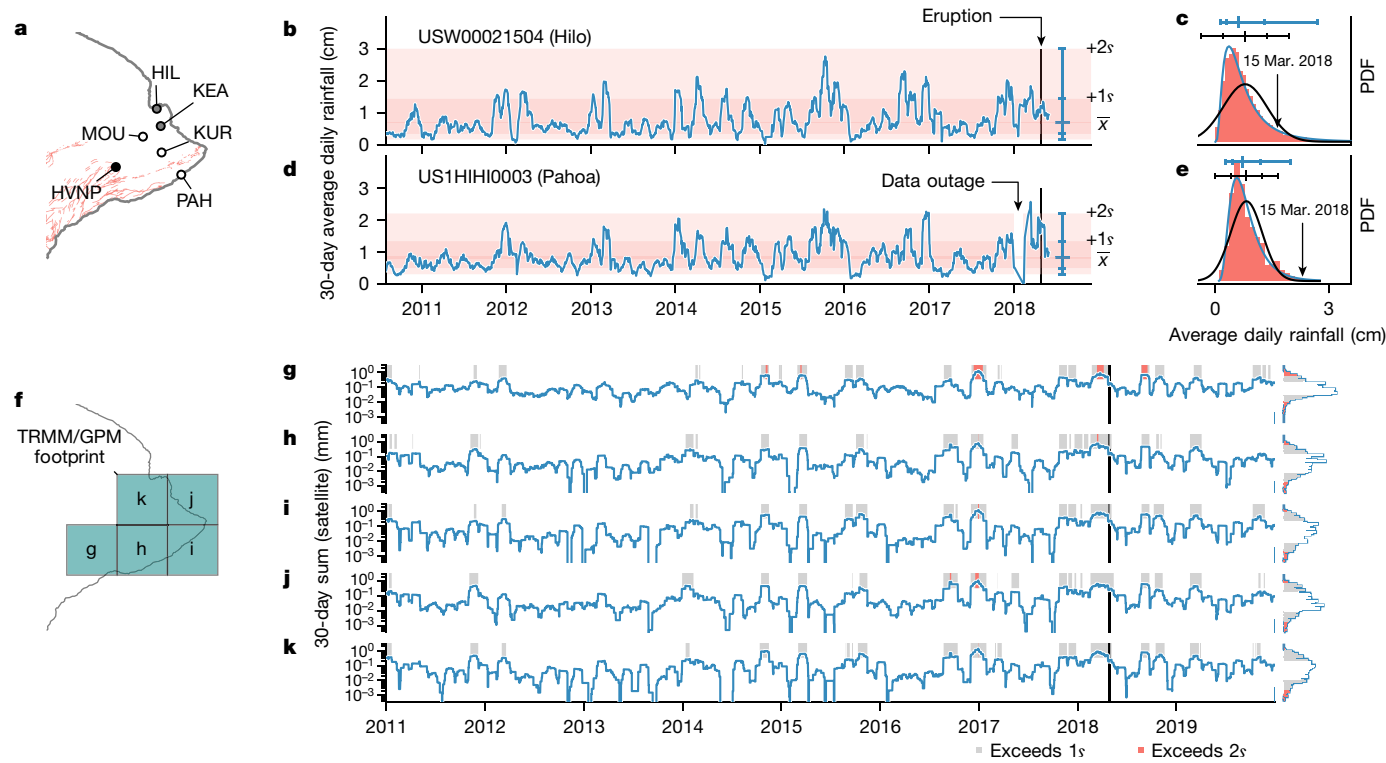


Fig. 1 | Pre-eruptive rainfall data. **a**, Location map showing gauges in the vicinity of the rift zone (fault system shown in red). HIL, Hilo International Airport (gauge USW00021504); KEA, Kea'au (USC00517023, USC00513872); KUR, Kurtistown (US1HIHI0055); MOU, Mountain View (US1HIHI0060, USC00516552); PAH, Pahoa (US1HIHI0008, US1HIHI0051, US1HIHI0003, USC00517457); HVNP, Hawai'i Volcanoes National Park (USC00511303).

b, Thirty-day running average time series of Hilo gauge data. Solid vertical line indicates 2018 intrusion date. Mean (\bar{x}) and standard deviations ($+1\sigma$, $+2\sigma$) are highlighted, based on lognormal relationship shown in **c**. **c**, Probability density function (PDF) of Hilo gauge data from 1 Oct 1949 until 1 June 2018. Solid black and blue curves are best-fit normal and lognormal functions, respectively. Ticked black and blue lines at top of panel highlight -2σ , -1σ , \bar{x} , $+1\sigma$ and $+2\sigma$

(iv) Furthermore, the lava lake level increase before the 2018 intrusion of 20–30 m is substantially smaller than the ~100-m increase before the 2011 intrusion (associated with the same ‘flow constriction’ mechanism¹² posited here by Poland et al.) or even the ~50-m increase of large deflation–inflation events¹³.

On the basis of recorded GPS displacements, Poland et al.¹ argue that there was substantial widespread pressurization before the 2018 intrusion. However, when viewed in the context of InSAR and geodetic data associated with both previous intrusions and periods of quiescence, the observed 2018 ground deformation was slight, altogether painting a picture of subtle and localized pressurization with a relatively minor effect on the volcanic edifice as a whole, particularly in the area where the 2018 intrusion initiated. Limited pressurization is characteristic of an ‘open’ magmatic system by definition. Nevertheless, we agree that the lake level increase indicates magma pressure increase and that it probably contributed to reaching the failure stress for dyke injection, while acknowledging that the relation between head change, magma pressure change and stress transfer into the edifice is complex owing to factors such as stratification and the presence of voids^{11,14}. However, the effect of any subtle pressure increase on the stress regime in the edifice was local, whereas the infiltrated precipitation affects the rock strength throughout the edifice. In contrast to the situation in the early 2018 period, the inflation of the much larger south caldera reservoir to June 2017 resulted in 45-cm inflation and stress changes within a larger portion of the edifice. The difference in stress state between 2011 and

distribution for either function. The 30-day average value two weeks before eruption is highlighted with an arrow. **d**, As **b**, for Pahoa gauge US1HIHI0003. **e**, As **c**, for Pahoa gauge between 1 July 2009 and 1 June 2018. **f**, Location map showing the footprints of five satellite data grids. **g–k**, Uncalibrated 30-day totals for different TRMM/Global Precipitation Measurement Mission (GPM) grid cells (**f**). For each time series, periods in which the windowed data exceed 1 and 2 standard deviations above the mean are highlighted. Marginal plots show histograms of windowed rainfall data, demonstrating the underlying lognormal distribution from which standard deviations are obtained (data from 2000 to 2020). Note that in early 2018, the rainfall signal is in all cases significantly greater than the mean at either the 1 or 2 σ level.

2018 highlighted by Poland et al. could reasonably be explained by inflation over this 2015–2017 period, along with ongoing progressive weakening of the edifice¹⁵.

Choosing a different seasonal threshold, Poland et al. refute any significant long-term correlation between rain and eruptions at Kilauea. Poland et al. assert that the correct threshold should be November–April, based on ref.¹⁶, a point with which we disagree. Their argument does not accurately represent the previous work¹⁶: seasons proposed by ref.¹⁶ are defined a priori and comprise an average for the entire state of Hawai'i. Moreover, those authors explicitly emphasize that ‘windward areas’ are an exception to the general annual rainfall cycle, indicating that the rift zone is not described by a November–April rainy season. In assuming this six-month season, the approach of Poland et al., to use their own words, “does not account for the complex patterns of rainfall and eruptions at Kilauea”¹. Our Fourier-based approach separates the periods of highest and least rainfall localized to the region of interest, which we deem preferable to a state-wide average known not to represent the rift zone.

We have not attempted to capture the complexity associated with defining the onset of previous eruptions (for example, “...several dyke intrusions”), instead using the published start dates from the Smithsonian Institution¹⁷, which do not necessarily include precursory non-eruptive volcanic activity. This does not detract from the observation that intrusions into the rift zone appear to be approximately twice as likely to occur when subsurface pressure perturbations are

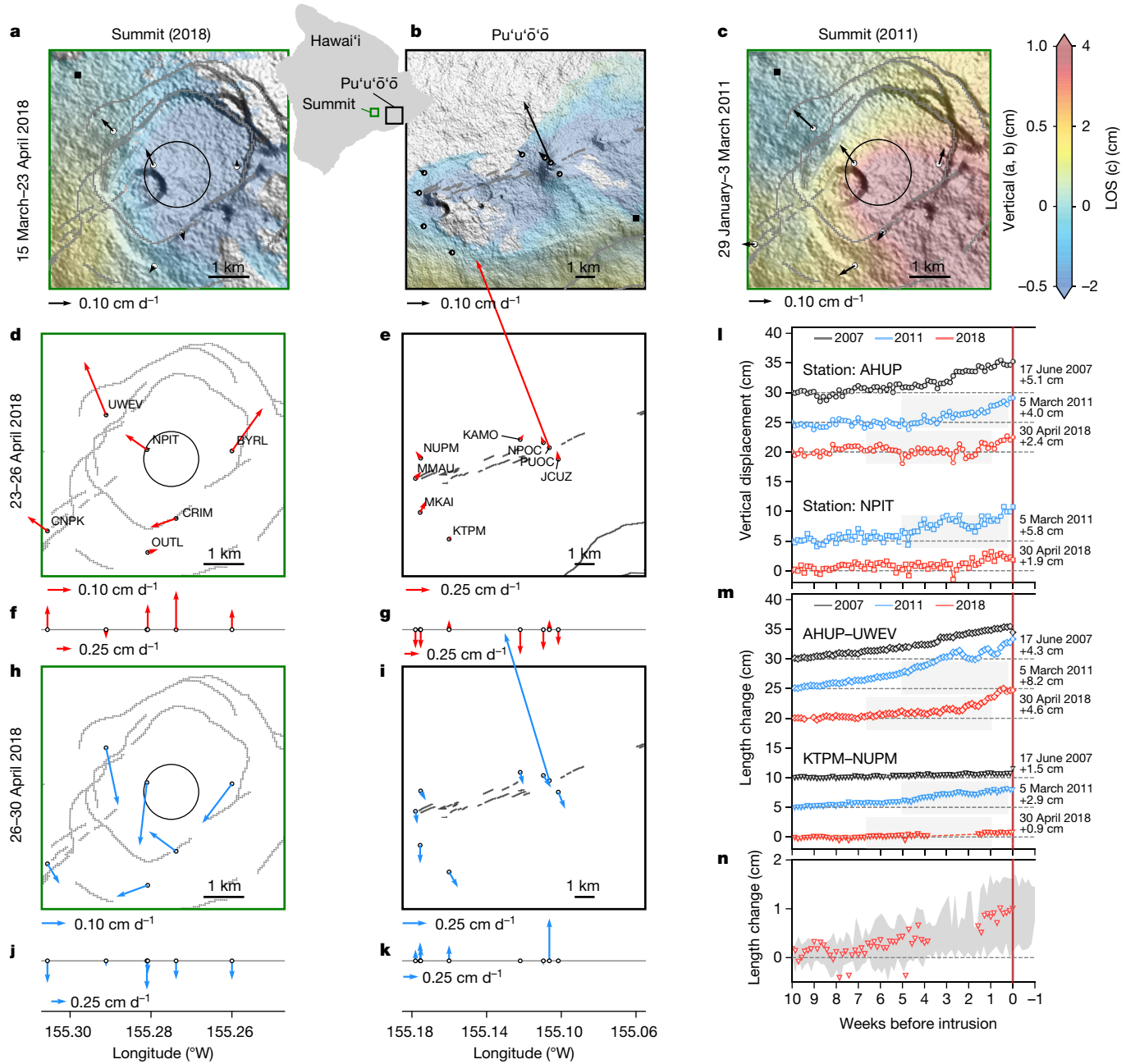


Fig. 2 | Precursory ground deformation at Kilauea. **a, b**, Vertical displacement determined from Sentinel-1InSAR data (ascending track 124 and descending track 87) for -15 March 2018 to -23 April 2018 (ascending: 15 March to 20 April 2018; descending: 18 March to 23 April 2018) at Kilauea's summit (**a**), and the Pu'u 'ō'ō region (**b**), together with horizontal GPS displacement vectors. Circle shows the estimated centroid location of the Halema'uma'u magma source. Black square is reference pixel. **c**, Line-of-sight (LOS) displacement (Cosmo-Skymed descending track 165) between 29 January and 2 March 2011. **d**, Horizontal GPS displacement between 23 April and 26 April at the summit. **e**, As **d**, for the Pu'u 'ō'ō region. **f**, Vertical GPS displacement at the summit between 23 and 26 April. **g**, As **f**, for Pu'u 'ō'ō. **h**, Horizontal GPS displacement between 26 and 30 April at the summit. **i**, As **h**, for Pu'u 'ō'ō. **j**, Vertical GPS displacement at the summit between 26 and 30 April. **k**, As **j**, for Pu'u 'ō'ō.

l, GPS time series for stations AHUP and NPIT, showing the vertical displacement before intrusions in 2007, 2011 and 2018. Solid vertical line represents intrusion. Annotations indicate intrusion dates and net displacement over the 10 weeks before. **m**, Line-length change between stations AHUP and UWEV (summit) and KTPM and NUPM (mid-rift), showing extensive displacement before intrusions in 2007, 2011 and 2018. **n**, Detailed view of length change between KTPM and NUPM stations. Red triangles show 2018 data and grey shaded region shows the range of evolution over the same months in previous years (2010, 2012–2017). Data for CNPK unavailable for time period in **a**. In **l**, **m**, time series data are offset from the x-axis for clarity, the shaded area indicates the corresponding InSAR epoch, and annotations indicate intrusion dates and net displacement over the 10 weeks before.

elevated above the running mean. Note that a significant correlation between rainfall and eruptions was reported in a previous U.S. Geological Survey study¹⁸, although dismissed at the time because it was “difficult to imagine a physical triggering mechanism of rainfall on eruptions”.

Poland et al. question the magnitude of computed rainfall-induced stress changes, suggesting that edifice fluid will be supercritical (thus, compressible) and that our permeability values are inappropriate. They also state that tide-induced pressure changes are greater than rainfall-induced perturbations.

Matters arising

While our stress changes are indeed small, this is probably often the case for eruption trigger stresses¹⁹; stress changes of 0.1–1 kPa are sufficient to induce failure in pre-stressed geological materials²⁰. Temperatures for supercriticality are maintained only in the immediate vicinity of a magma body²¹, whereas the mechanical influence of pore fluid can extend throughout the edifice. Our shallow permeability values are in line with recent studies of Kilauea²².

Theoretical tidal displacements at Kilauea between April and June 2018 could effect positive pore pressure changes of at most around 0.1 kPa assuming realistic (poro-)elastic parameters (for example, elastic moduli²³; Biot coefficient²⁴). Moreover, Poland et al. draw a false equivalence here: stress perturbations required for mechanical failure by (high-frequency, short-period) dynamic stressors are higher than those required for static or quasi-static stresses²⁵, as we state in our Article.

As a final note, we highlight that Poland et al. refer to four articles that were unpublished and thus unavailable at the time of writing; indeed, one of these is a solicited News & Views piece that accompanied our original Article.

Data availability

All data are open source. Satellite-derived rainfall data (TRMM and GPM satellite data) are available from the NASA (National Aeronautics and Space Administration) EarthData Goddard Earth Sciences Data and Information Services Center portal (<https://doi.org/10.5067/TRMM/TMPA/3H/7>). Rainfall gauge data are available from the National Oceanic and Atmospheric Administration's National Centers for Environmental Information climate data portal (<https://www.ncdc.noaa.gov/cdo-web/datasets/GHCND/stations/GHCND:USC00511303/detail>). GPS data are available from the Nevada Geodetic Laboratory (<http://geodesy.unr.edu/NGLStationPages/stations/>). Sentinel-1 ascending- and descending-track SAR acquisitions were obtained through UNAVCO's Seamless SAR Archive (<https://doi.org/10.5194/isprsarchives-XL-1-65-2014>). Derived time series products of Kilauea are available at <https://doi.org/10.5281/zenodo.3944709> and <https://doi.org/10.5281/zenodo.3957859>.

Code availability

Code required for data access, analysis and display is available, in Jupyter Notebook format, at https://github.com/jifarquharson/Farquharson_Amelung_2020_Kilauea-Nature/blob/master/Farquharson_Amelung_Kilauea_Supplemental_2.ipynb (Fig. 1) and https://github.com/jifarquharson/Farquharson_Amelung_2020_Kilauea-Nature/blob/master/Farquharson_Amelung_Kilauea_Supplemental_1.ipynb (Fig. 2).

1. Poland, M. P. et al. Rainfall an unlikely factor in Kilauea's 2018 rift eruption. *Nature* <https://doi.org/10.1038/s41586-020-2172-5> (2022).
2. Farquharson, J. I. & Amelung, F. Extreme rainfall triggered the 2018 rift eruption at Kilauea Volcano. *Nature* **580**, 491–495 (2020).
3. Farquharson, J. I. & Amelung, F. Author Correction: Extreme rainfall triggered the 2018 rift eruption at Kilauea Volcano. *Nature* **582**, E3 (2020).
4. Dzurisin, D. Influence of fortnightly earth tides at Kilauea Volcano, Hawaii. *Geophys. Res. Lett.* **7**, 925–928 (1980).

5. Lipman, P. W., Lockwood, J. P., Okamura, R. T., Swanson, D. A. & Yamashita, K. M. *Ground Deformation Associated with the 1975 Magnitude-7.2 Earthquake and Resulting Changes in Activity of Kilauea Volcano, Hawaii* (1985).
6. Poland, M. P., Sutton, A. J. & Gerlach, T. M. Magma degassing triggered by static decompression at Kilauea Volcano, Hawai'i. *Geophys. Res. Lett.* **36**, L16306 (2009).
7. Orr, T. R., Thelen, W. A., Patrick, M. R., Swanson, D. A. & Wilson, D. C. Explosive eruptions triggered by rockfalls at Kilauea volcano, Hawai'i. *Geology* **41**, 207–210 (2013).
8. *Volcano Hazards Program FAQs* (USGS, 2011); https://volcanoes.usgs.gov/vsc/file_mngr/file-153/FAQs.pdf
9. Oosterbaan, R. J. in *Vol. 16* 175–224 (IILRI, 1994).
10. Chen, Y., Ebert, E. E., Walsh, K. J. E. & Davidson, N. E. Evaluation of TRMM 3B42 precipitation estimates of tropical cyclone rainfall using PACRAIN data. *J. Geophys. Res. Atmos.* **118**, 2184–2196 (2013).
11. Bagnardi, M. et al. Gravity changes and deformation at Kilauea Volcano, Hawaii, associated with summit eruptive activity, 2009–2012. *J. Geophys. Res. Solid Earth* **119**, 7288–7305 (2014).
12. Patrick, M. R., Anderson, K. R., Poland, M. P., Orr, T. R. & Swanson, D. A. Lava lake level as a gauge of magma reservoir pressure and eruptive hazard. *Geology* **43**, 831–834 (2015).
13. Anderson, K. R., Poland, M. P., Johnson, J. H. & Miklius, A. in *Hawaiian Volcanoes* 229–250 (American Geophysical Union, 2015).
14. Parfitt, L. & Wilson, L. *Fundamentals of Physical Volcanology* (Wiley, 2009).
15. Wauthier, C., Roman, D. C. & Poland, M. P. Modulation of seismic activity in Kilauea's upper East Rift Zone (Hawai'i) by summit pressurization. *Geology* **47**, 820–824 (2019).
16. Frazier, A. G. & Giambellucca, T. W. Spatial trend analysis of Hawaiian rainfall from 1920 to 2012. *Int. J. Climatol.* **37**, 2522–2531 (2017).
17. *Global Volcanism Program*, 2013. *Volcanoes of the World Version 4.9.1* (accessed 17 September 2020); <https://doi.org/10.5479/si.GVPVOTW4-2013>.
18. Klein, F. W. Eruption forecasting at Kilauea Volcano, Hawaii. *J. Geophys. Res. Solid Earth* **89**, 3059–3073 (1984).
19. Díez, M., Femina, P. C. L., Connor, C. B., Strauch, W. & Tenorio, V. Evidence for static stress changes triggering the 1999 eruption of Cerro Negro Volcano, Nicaragua and regional aftershock sequences. *Geophys. Res. Lett.* **32**, L04309 (2005).
20. Hainzl, S., Kraft, T., Wassermann, J., Igel, H. & Schmedes, E. Evidence for rainfall-triggered earthquake activity. *Geophys. Res. Lett.* **33**, L19303 (2006).
21. Hayba, D. O. & Ingebritsen, S. E. Multiphase groundwater flow near cooling plutons. *J. Geophys. Res. Solid Earth* **102**, 12235–12252 (1997).
22. Hsieh, P. A. & Ingebritsen, S. E. Groundwater inflow toward a preheated volcanic conduit: application to the 2018 eruption at Kilauea Volcano, Hawai'i. *J. Geophys. Res. Solid Earth* **124**, 1498–1506 (2019).
23. Heap, M. J. et al. Towards more realistic values of elastic moduli for volcano modelling. *J. Volcanol. Geotherm. Res.* **390**, 106684 (2020).
24. Farquharson, J., Heap, M. J., Baud, P., Reuschlé, T. & Varley, N. R. Pore pressure embrittlement in a volcanic edifice. *Bull. Volcanol.* **78**, 6 (2016).
25. Li, D., Wang, T., Cheng, T. & Sun, X. Static and dynamic tensile failure characteristics of rock based on splitting test of circular ring. *Trans. Nonferrous Met. Soc. China* **26**, 1912–1918 (2016).

Acknowledgements Copernicus Sentinel-1 and Cosmo-Skymed SAR data are available thanks to the Group on Earth Observation's Geohazard Supersites and Natural Laboratory Initiative. This work was supported by funding from NASA's Interdisciplinary Research in Earth Science programme (grant number 80NSSC17K0028 P00003). Data processing was conducted using Stampede2 at the Texas Advanced Computing Center of the Extreme Science and Engineering Discovery Environment, supported by National Science Foundation grant number ACI-1548562, using the public domain InSAR Scientific Computing Environment software of the Jet Propulsion Laboratory. We thank B. Varugu for discussions.

Author contributions J.I.F. processed the GPS and rainfall data, and plotted all data. F.A. processed the InSAR data. Both authors contributed to the writing.

Competing interests This work was supported by funding from NASA's Interdisciplinary Research in Earth Science programme (grant number 80NSSC17K0028 P00003) exploring the influence of rainfall in triggering volcanism.

Additional information

Correspondence and requests for materials should be addressed to Jamie I. Farquharson. **Reprints and permissions information** is available at <http://www.nature.com/reprints>. **Publisher's note** Springer Nature remains neutral with regard to jurisdictional claims in published maps and institutional affiliations.

© The Author(s), under exclusive licence to Springer Nature Limited 2022